Journal of Zhejiang University-SCIENCE C (Computers & Electronics)
ISSN 1869-1951 (Print); ISSN 1869-196X (Online)
www.zju.edu.cn/jzus; www.springerlink.com
E-mail: jzus@zju.edu.cn

Exploring the mechanism of neural-function reconstruction by reinnervated nerves in targeted muscles*

Hui ZHOU[1], Lin YANG[1], Feng-xia WU[1], Jian-ping HUANG[1],
Liang-qing ZHANG[1,2], Ying-jian YANG[1,3], Guang-lin LI[†‡1]

([1]*Institute of Biomedical and Health Engineering, Shenzhen Institutes of Advanced Technology, Chinese Academy of Sciences, Shenzhen 518055, China*)

([2]*Department of Rehabilitation Medicine, Nanshan Hospital Affiliated to Guangdong Medical College, Shenzhen 518052, China*)

([3]*Sino-Dutch Biomedical and Information Engineering School of Northeastern University, Shenyang 110004, China*)

[†]E-mail: gl.li@siat.ac.cn

Received Apr. 26, 2014; Revision accepted July 13, 2014; Crosschecked Sept. 17, 2014

Abstract: A lack of myoelectric sources after limb amputation is a critical challenge in the control of multifunctional motorized prostheses. To reconstruct myoelectric sources physiologically related to lost limbs, a newly proposed neural-function construction method, targeted muscle reinnervation (TMR), appears promising. Recent advances in the TMR technique suggest that TMR could provide additional motor command information for the control of multifunctional myoelectric prostheses. However, little is known about the nature of the physiological functional recovery of the reinnervated muscles. More understanding of the underlying mechanism of TMR could help us fine tune the technique to maximize its capability to achieve a much higher performance in the control of multifunctional prostheses. In this study, rats were used as an animal model for TMR surgery involving transferring a median nerve into the pectoralis major, which served as the target muscle. Intramuscular myoelectric signals reconstructed following TMR were recorded by implanted wire electrodes and analyzed to explore the nature of the neural-function reconstruction achieved by reinnervation of targeted muscles. Our results showed that the active myoelectric signal reconstructed in the targeted muscle was acquired one week after TMR surgery, and its amplitude gradually became stronger over time. These preliminary results from rats may serve as a basis for exploring the mechanism of neural-function reconstruction by the TMR technique in human subjects.

Key words: Neural function reconstruction, Targeted muscle reinnervation, Intramuscular myoelectric signal, Myoelectric prostheses

doi:10.1631/jzus.C1400154 **Document code:** A **CLC number:** TP212.3; Q189

1 Introduction

Limb amputees expect to have a reliable and easy-to-use motorized prosthesis for doing various tasks in their daily lives. Much has been done to improve continuously the performance of multifunctional myoelectric prostheses (Parker and Scott, 1986; Hudgins *et al.*, 1993; Ajiboye and Weir, 2005; Huang *et al.*, 2005). However, the control of multifunctional prostheses is still limited due to a lack of myoelectric sources after limb amputations. This issue is more critical for high-level limb amputees since little or no muscle may remain on their residual limbs to provide enough electromyography (EMG) signals for the proper control of multifunctional prostheses. Recently, a new neural-machine interface called targeted muscle reinnervation (TMR) has been proposed in an attempt to reconstruct EMG sources lost in limb

‡ Corresponding author

* Project supported by the National Basic Research Program (973) of China (No. 2013CB329505), the National Natural Science Foundation of China (Nos. 61135004 and 61201114), the China Postdoctoral Science Foundation (No. 2013M541046), the Shenzhen Governmental Basic Research Grant (No. JCYJ20120617115010496), and the State Key Laboratory of Bioelectronics of Southeast University

amputations (Kuiken *et al.*, 2007; 2009; Miller *et al*., 2008; Li *et al*., 2010). TMR is a surgery technique that transfers the remaining limb nerves to available skeletal muscles of a limb amputee. These reinnervated muscles are called targeted muscles and may no longer be physiologically functional after limb amputations. After TMR surgery, the residual nerves reinnervate the targeted muscles over time, and then the reinnervated muscles provide myoelectric signals which are biologically associated with the original movements in the missing limbs of the amputees.

Recent advances in the technique suggest that TMR could provide additional motor command information for the control of multifunctional myoelectric prostheses (Zhou *et al*., 2007). While these studies have shown that TMR has the ability to improve significantly the control performance of myoelectric artificial arms, investigations exploring the nature of neural-function reconstruction by TMR would be valuable. With more understanding of the underlying mechanism of TMR, we could fine tune the TMR technique to maximize its capability to achieve a much higher performance in the control of multifunctional prostheses. Although TMR has been proposed and investigated for around a decade, the nature of the physiological functional recovery of the reinnervated muscles is largely unknown. Only two relevant studies have been conducted in an attempt to explore the underlying mechanism of TMR. Stubblefield *et al*. (2009) found that a tiny twitch could be first felt and observed with a TMR interface from 10 to 15 weeks after TMR. Our previous pilot study on a rat TMR model showed that a reinnervated nerve had re-grown into the targeted muscle, and that intramuscular myoelectric signals could be captured with implanted wire electrodes from the reinnervated muscle about one week after TMR (Zhou *et al*., 2013). However, it is still unclear how myoelectric activities are changed during the reinnervation process after TMR. A previous study showed that the regeneration of injured nerves may not depict muscle function recovery properly (Sabatier *et al*., 2011). Thus, for the TMR technique, there is still a lack of detailed myoelectric information regarding this recovery process. Obviously, it is inappropriate to conduct these kinds of investigations on human subjects who have had TMR surgery. Therefore, using a fast and reliable evaluation method to assess the nature of the muscle functional recovery process after TMR surgery is necessary, and will provide a basis for further improvement of the TMR technique and its application in clinical treatments.

In this study, we used rats as an animal model to develop TMR surgery by transferring a median nerve into the pectoralis major, which served as the targeted muscle. Then, intramuscular myoelectric signals were recorded with wire electrodes implanted into the reinnervated muscle and the underlying mechanism of the functional recovery of the reinnervated muscle was explored by analysis of the myoelectric signals. A Morlet-wavelet-based EMG intensity analysis algorithm was adopted (Mummidisetty, 2009) to detect the start and end of myoelectric activity. The active myoelectric signals could then be extracted from the signal recordings for further analysis. This pilot study on rats provides some valuable information which can be used to explore the mechanism of neural-function reconstruction by the TMR technique in human subjects.

2 Materials and methods

2.1 General animal procedures

Twelve Sprague-Dawley rats (specific pathogen-free level, provided by the Guangdong Medical Laboratory Animal Center) with a weight range of 200–250 g were used. All the rats were housed in a temperature and humidity controlled room with a 12-h day/night cycle and access to food and water ad libitum. The rats were randomly assigned to two groups: a targeted muscle reinnervation (TMR) group (n=6) and a denervation group (n=6). For the rats in the TMR group, the pectoralis major muscle on the right side of the chest was selected as the reinnervated muscle. For the rats in the denervation group, the original innervated nerves of the pectoralis major muscle on the right side were transected by surgery, but had no nerve transfer. The pectoralis major muscle on the left side in rats of the two groups remained intact for comparison. All the animal experimental procedures were approved by the Ethics Committee for Animal Research, Shenzhen Institutes of Advanced Technology, Chinese Academy of Sciences.

2.2 Rat models with TMR

TMR surgery was performed on the right side of the pectoralis major muscle of each of the six rats in the TMR group. The procedure was similar to that described in a previous study (Zhou *et al.*, 2013). Briefly, before the surgery, an anesthetic procedure was conducted on the rats using 10% chloral hydrate (0.3/100 g) through intraperitoneal injection. A depilatory cream was used after shaving the right anterior thorax, shoulder girdle, and entire right forelimb of each rat. Then, povidoneiodine and 75% alcohol were used to sterilize the surgical region of the skin. Each rat was incised over a continuous '┐' shaped region starting from the right forelimb cubital fossa and along the axillary fold to the chest. The dissection was performed carefully to identify and expose the median nerve and ulnar nerve (medial side) structures, as they exited the brachial plexus. The median nerve was detached and cut inside the cubital fossa. Denervation of the right side pectoralis muscle was achieved by transecting the original innervating nerves (Kuiken *et al.*, 2004; Hijjawi *et al.*, 2006). Note that this denervation procedure was also used for the six rats in the denervation group. For nerve reinnervation, 10-0 nylon sutures were used to transfer the remnant median nerve into the pectoralis major muscle. After completing the surgical process, 4-0 sutures were used to close the skin incision, layer by layer.

2.3 Implantation of intramuscular myoelectric electrodes

Intramuscular myoelectric signals were recorded with five stainless steel wires that were connected to the targeted muscle of the rats via a connector on the head (Figs. 1 and 2). The wire electrodes and head connector were implanted following the protocols of Roy *et al.* (1991), Tysseling *et al.* (2013), and Zhou *et al.* (2013). In brief, a 5-pin connector (Omnetic, Minneapolis, MN, USA) was secured to the skull, and Teflon-coated stainless wires (Cat No. 793500, A-M System Inc.) were passed subcutaneously to the back or the pectoralis muscle. Teflon insulation on the 2-mm long tip of the stainless wire was removed to form the recording electrode. Fig. 1a illustrates the settlement of the head connector. After the Omnetic connector had been properly cemented to the skull and screws, sutures were used to close the incisions between the dental cement and the skull skin (Fig. 1b).

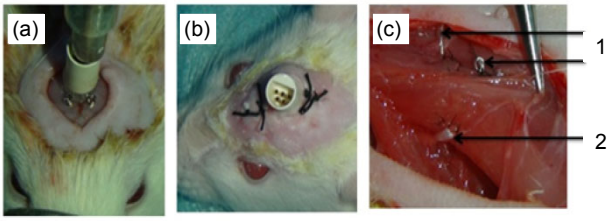

Fig. 1 Head connector and intramuscular electrodes in a TMR rat
(a) shows the head connector before cementation; in (b), the incision between the dental cement and the skull skin was closed with sutures; in (c), number 1 denotes the implanted intramuscular electrodes and number 2 the transferred median nerve

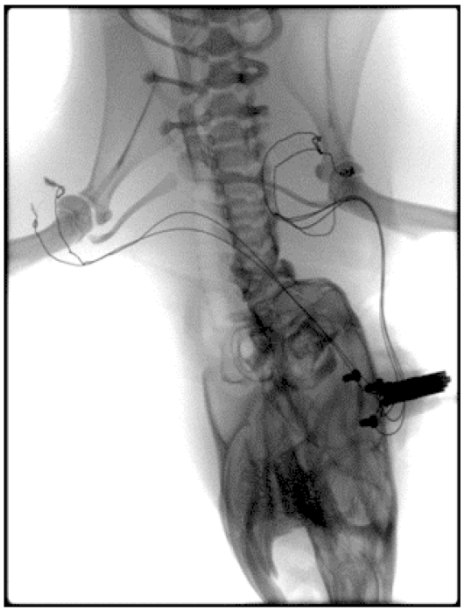

Fig. 2 Micro-focus X-ray image of a rat with implanted intramuscular electrodes and a head connector

A picture of the implanted wire electrodes and the transferred nerve in one TMR rat is shown in Fig. 1c. A micro-focus X-ray image was used to verify further the position of the electrode within the rats after its implantation (Fig. 2). The implanted wire electrodes are shown properly positioned in the pectoralis major muscle on both sides, while the ground electrode is located under the skin near the neck.

2.4 Acquisition of intramuscular myoelectric signals

When the rats were walking on a treadmill, a biological signal acquisition system (MedLab-

U8C502, Nanjing MedEase Science and Technology Co., Ltd., China) with a 1-m long cable was used to record intramuscular myoelectric signals that could induce contraction of the targeted muscle. After the surgery, treadmill mobility and myoelectric signal recording experiments were performed once per week over four weeks. For each rat, the experiment was composed of three trials, each with a 30-s running session and then a 30-s rest session. A belt speed of 9 m/min with a 15° incline was set during the treadmill mobility experiments. The myoelectric signals were amplified with a gain of 1000 and then recorded at a sample rate of 2000 Hz. According to the power spectral analysis of the myoelectric signal recordings, components with a frequency of around 100 Hz and below were mainly noise and interference, so a high pass filter of 125 Hz was used in this study.

2.5 Analysis of intramuscular myoelectric signals

The signal recordings included myoelectric signals during active contractions of the reinnervated muscle and signals during muscle inactivity, such as interference, noise, and movement artifacts (Fig. 3). To evaluate muscle functional recovery, the active myoelectric signals from reinnervated muscle needed to be extracted from the recordings. The myoelectric intensity analysis methods proposed by von Tscharner (2000) and Mummidisetty (2009) were adopted to detect the onset and offset of the active myoelectric signals. Briefly, four steps were used to mark the active myoelectric onset and offset times. The first step was to create filter banks based on Morlet wavelets. Seventeen filter banks were used to cover the entire myoelectric frequency range of 0 to 1000 Hz. In the second step, the developed filter banks were used to obtain 17 envelops of myoelectric signals, and then only those envelopes in intermediate frequencies were combined to detect the onset and offset times of myoelectric signals. According to Mummidisetty (2009), the intermediate frequency bands are more sensitive to myoelectric changes and better for avoiding multiple myoelectric peaks than other frequency bands. Thus, intermediate frequency bands were adopted to calculate onset and offset times. Thirdly, the peaks of the combined envelope were automatically annotated, and then those caused by artifact or noise were manually removed according to some raw myoelectric recordings. Each peak represented an active contraction of the targeted muscle. Finally, for each peak, the onset and offset of the active contraction was determined according to the energy distribution of an analysis window around the peak in the combined envelope. The analysis window was centered in the peak and had a total length of 300 ms. The onset was defined as the time corresponding to 10% of the total energy, and the off time was defined as the time corresponding to 90% of the total energy.

In the analysis of myoelectric signals, a measure called the average rectified value (ARV) of the active myoelectric signals was used to characterize the activity levels of the targeted muscle. The ARV was defined as

$$\frac{1}{T}\int_0^T |X(t)|\mathrm{d}t,$$

which is a time-windowed mean of the absolute value of an active myoelectric signal. Statistical analyses of ARV values were performed using SPSS 13.0 software, in which a paired *t*-test analysis was applied to determine the statistical significance of differences between the same muscles at different times. The significance threshold was set at $P<0.05$. All statistical results were expressed as mean±S.E.M.

3 Results

3.1 General animal procedures

Active myoelectric signals of the targeted muscles were successfully acquired with the implanted wire electrodes from all 12 rats in the two groups. Fig. 3 shows some typical waveforms of intramuscular myoelectric activity from one rat in the reinnervation group and another in the denervation group when walking on the treadmill. For each rat, the myoelectric signals from both the post-operative and intact sides of the pectoralis major muscles are represented in Fig. 3. For the TMR rat, Fig. 3a (two upper rows) shows that its reinnervated muscle, which was the right side of the pectoralis, began producing some weak myoelectric signal one week post-surgery, when walking on the treadmill. In the fourth week after TMR surgery, the intramuscular myoelectric signal from its reinnervated muscle became much stronger with an amplitude comparable to that of its intact

pectoralis (left side). For the denervated rat, normal myoelectric activities were recorded from its intact pectoralis muscle, but were mostly absent from its denervated muscle, when walking on treadmill (Fig. 3b). Similar results were observed from all the rats in the TMR and denervation groups.

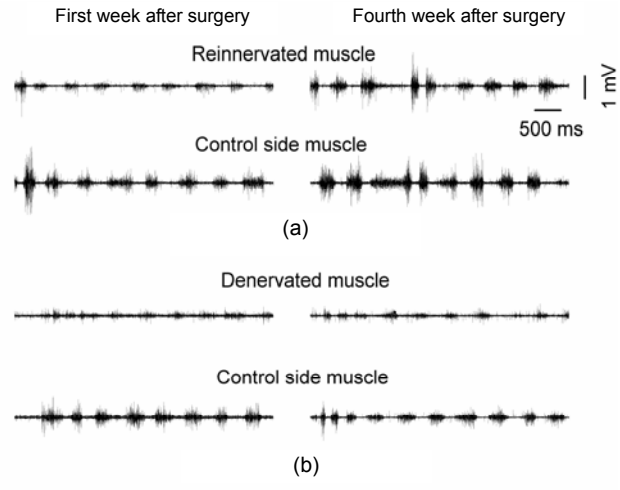

Fig. 3 Typical waveforms of intramuscular myoelectric signals from the targeted muscles of rats in the first and fourth weeks after surgery: (a) intramuscular myoelectric signal recordings from a TMR rat; (b) intramuscular myoelectric signal recordings from a denervated rat

3.2 Extraction of active myoelectric signals

Only myoelectric signals from the activities of the targeted muscles were required for statistical analysis. These signals were extracted using a Morlet-wavelet-based algorithm when the rats were walking on the treadmill. Table 1 shows the central frequencies corresponding to Morlet wavelet indexes of from 0 to 17. When the Morlet wavelet index was greater than 16, the central frequency was greater than 1000 Hz.

With a sampling rate of 1000 Hz, only Morlet wavelet banks with an index of from 0 to 16 were calculated and included (Fig. 4). Envelopes in low-frequency bands included little useful information and those in high-frequency bands presented a number of peaks in one active contraction of muscle. Thus, the four envelopes with an index range of 9 to 12 were added together to obtain a new envelope of intermediate frequency bands, as suggested by Mummidisetty (2009). The envelope of intermediate frequency bands was then used to automatically mark the active myoelectric peaks. A representative figure showing the detection of active myoelectric peaks is illustrated in Fig. 5. All the peaks could be accurately annotated using the proposed method. Based on these annotated peaks, the onset and offset of the active contractions were successfully determined, and the active myoelectric signals between the onset and offset were extracted from signal recordings for statistical analysis.

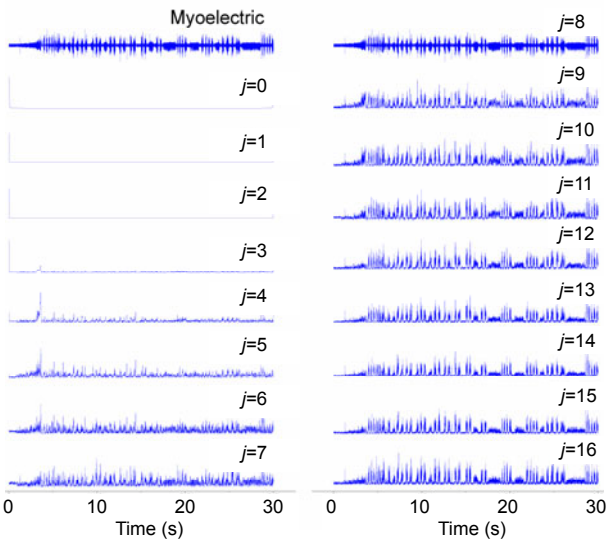

Fig. 4 Myoelectric envelopes computed by the Morlet wavelet at 17 central frequencies

Table 1 The Morlet wavelet indexes and their corresponding central frequencies

Wavelet index	Central frequency (Hz)	Wavelet index	Central frequency (Hz)	Wavelet index	Central frequency (Hz)
0	6.9024	6	170.3856	12	542.0579
1	19.2866	7	218.0675	13	623.8208
2	37.7109	8	271.4874	14	711.1966
3	62.0892	9	330.6188	15	804.1698
4	92.3591	10	395.4383	16	902.7261
5	128.4713	11	465.9245	17	1006.9000

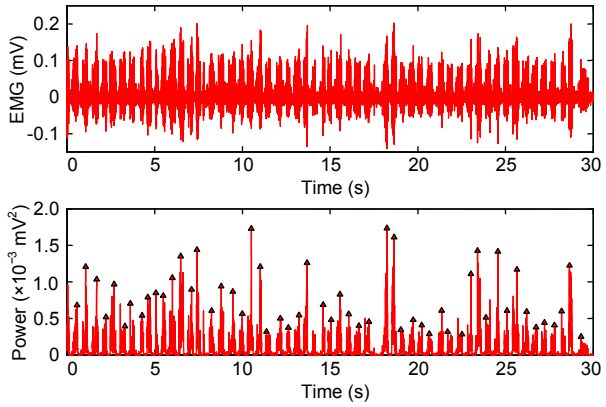

Fig. 5 A representative myoelectric signal and its burst peaks: (a) myoelectric signal from a rat; (b) the developed power (square of envelopes) with the burst peaks being marked by triangle symbols

3.3 Analysis of active myoelectric signals

The analysis was conducted on the ARVs of the active myoelectric signals from all the rats. Fig. 6 shows the ARVs of myoelectric activities averaged over all six TMR rats. The upper row shows that the ARVs from the reinnervated muscle were gradually increasing from the first to the fourth week after TMR surgery, and that the difference between the first week and the fourth week was significant (P=0.006).

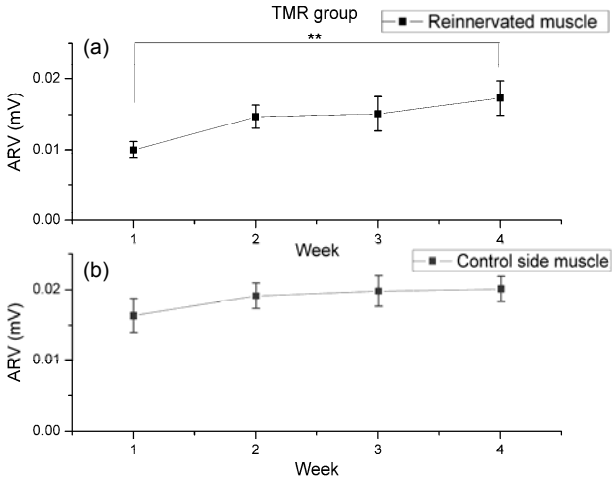

Fig. 6 ARVs of active myoelectric signals from both sides of the pectoralis averaged over the six TMR rats four weeks after surgery: (a) reinnervated muscle; (b) control side muscle

** indicates a significant difference between the first and fourth weeks. A paired t-test was used in the computation

For the intact pectoralis muscle, the ARVs of myoelectric activities averaged over the six rats also showed a slightly increasing trend, but did not show a significant difference between the first and the fourth weeks (P>0.05). For the rats in the denervation group, the ARVs of myoelectric activities averaged over the six rats showed a slight change over time for both the post-operative and intact pectoralis muscles (Fig. 7), but the difference between weeks was not significant.

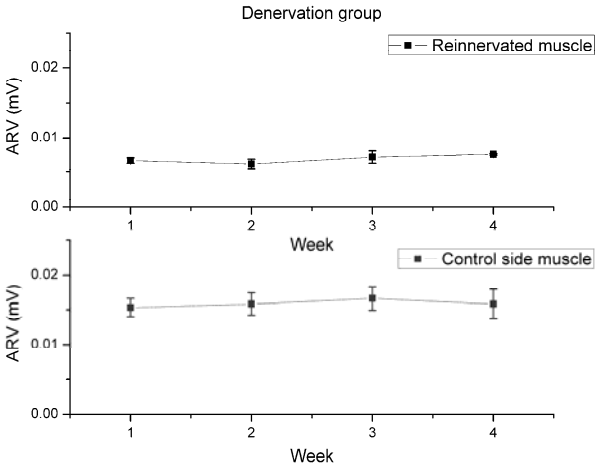

Fig. 7 ARVs of active myoelectric signals from both sides of the pectoralis averaged over the six denervated rats four weeks after surgery: (a) reinnervated muscle; (b) control side muscle

A paired t-test was used in the computation

4 Discussion

This study presented a statistical analysis of the active myoelectric signals in rats of a TMR group and a denervation group within four weeks after surgery. The reinnervated muscle showed a gradual increase in myoelectric activity while the denervated muscle showed little change from the first to the fourth week. This increase in myoelectric activity of reinnervated muscle suggests that a functional recovery may occur after reinnervation. For the recorded raw myoelectric signal, it was hard to detect this recovery process in all the rats. By using the method of detecting onset and offset times of active myoelectric signals and extracting myoelectric information from the signals between the onset and offset, a notable increase in myoelectric activity was apparent only in the reinnervated muscle. Myoelectric activity in the control

muscles was stronger in the TMR group than in the denervation group (Fig. 3). The amplitude of the recorded myoelectric signal depended on the efforts of the rats in walking. When the denervated muscle became weak in the fourth week, the rats may have made less effort in their control muscles to keep their body balance during walking. This might explain why the myoelectric signals from the intact muscles were stronger in the TMR group than in the denervation group. The proposed method might have potential for reliable and quantitative evaluation of muscle functional recovery for amputees after TMR surgery.

An intensity analysis based on the onset and offset calculation method was adopted in this study. Filter banks were first developed with wavelets at different central frequencies, and then the myoelectric signals were analyzed at these specific frequency bands. Annotation of the myoelectric peaks in the intermediate frequency bands may provide sensitivity to the myoelectric changes and be capable of avoiding the detection of multiple peaks during one active period. There are numerous methods of myoelectric onset and offset time detection (Staude *et al*., 2001; Li *et al*., 2007; Solnik *et al.*, 2008), which focus mainly on detecting myoelectric on and off times with accuracy. However, the intensity analysis based method used in this study focused on detecting the active myoelectric signal correctly, since there were many artifacts and noises between active myoelectric signals that may otherwise have been mistaken as active myoelectric signals.

Previous studies have reported that EMG activity can provide insights into the functional recovery process (English *et al.*, 2006; Hu *et al.*, 2009; Sabatier *et al.*, 2011). Further work will be done to associate the extracted active myoelectric information with other methods, such as H-flex, gait analysis, and BBB scores, to make the method used in this study reliable for assessing muscle function recovery. Implanted stainless wires were used for recording myoelectric signals in this study. The impedance between the electrode and the tissue might change after implantation over time. This change in impedance may influence the measured EMG amplitudes. Our statistical results showed a slightly increasing trend, but no statistically significant increase in myoelectric amplitude in control side muscles within four weeks. We will conduct further experiments to investigate the relationship between impedance changes and the myoelectric signal amplitude.

5 Conclusions

In this study, intramuscular myoelectric signals were recorded using wire electrodes implanted into the reinnervated muscle of rats, and the underlying nature of the functional recovery of reinnervated muscle was explored by analysis of the myoelectric signals. For the TMR rats, statistical analysis of extracted myoelectric information from active myoelectric signals between the onset and offset showed a gradual improvement in myoelectric activity, and a statistically significant difference was found between the fourth and the first weeks in the reinnervated muscle. The results from rats might be helpful for exploring the mechanisms of neural-function reconstruction by the TMR technique in human subjects.

References

Ajiboye, A.B., Weir, R.F., 2005. A heuristic fuzzy logic approach to EMG pattern recognition for multifunctional prosthesis control. *IEEE Trans. Neur. Syst. Rehabil. Eng.*, **13**(3):280-291. [doi:10.1109/TNSRE.2005.847357]

English, A.W., Chen, Y., Carp, J.S., *et al*., 2006. Recovery of electromyographic activity after transection and surgical repair of the rat sciatic nerve. *J. Neurophysiol.*, **97**(2): 1127-1134. [doi:10.1152/jn.01035.2006]

Hijjawi, J.B., Kuiken, T.A., Lipschutz, R.D., *et al*., 2006. Improved myoelectric prosthesis control accomplished using multiple nerve transfers. *Plast. Reconstr. Surg.*, **118**(7):1573-1578. [doi:10.1097/01.prs.0000242487.62487.fb]

Hu, X.L., Tong, K.Y., Song, R., *et al*., 2009. Quantitative evaluation of motor functional recovery process in chronic stroke patients during robot-assisted wrist training. *J. Electromyogr. Kinesiol.*, **19**(4):639-650. [doi:10.1016/j.jelekin.2008.04.002]

Huang, Y.H., Englehart, K.B., Hudgins, B., *et al*., 2005. A Gaussian mixture model based classification scheme for myoelectric control of powered upper limb prostheses. *IEEE Trans. Biomed. Eng.*, **52**(11):1801-1811. [doi:10.1109/TBME.2005.856295]

Hudgins, B., Parker, P., Scott, R.N., 1993. A new strategy for multifunction myoelectric control. *IEEE Trans. Biomed. Eng.*, **40**(1):82-94. [doi:10.1109/10.204774]

Kuiken, T.A., Dumanian, G.A., Lipschutz, R.D., *et al*., 2004. The use of targeted muscle reinnervation for improved myoelectric prosthesis control in a bilateral shoulder disarticulation amputee. *Prosthet. Orthot. Int.*, **28**(3):245-253.

Kuiken, T.A., Miller, L.A., Lipschutz, R.D., *et al.*, 2007. Targeted reinnervation for enhanced prosthetic arm function in a woman with a proximal amputation: a case study. *The Lancet*, **369**(9559):371-380. [doi:10.1016/S0140-6736(07)60193-7]

Kuiken, T.A., Li, G.L., Lock, B.A., *et al.*, 2009. Targeted muscle reinnervation for real-time myoelectric control of multifunction artificial arms. *JAMA*, **301**(6):619-628. [doi:10.1001/jama.2009.116]

Li, G.L., Schultz, A.E., Kuiken, T.A., 2010. Quantifying pattern recognition-based myoelectric control of multifunctional transradial prostheses. *IEEE Trans. Neur. Syst. Rehabil. Eng.*, **18**(2):185-192. [doi:10.1109/TNSRE.2009.2039619]

Li, X., Zhou, P., Aruin, A.S., 2007. Teager-Kaiser energy operation of surface EMG improves muscle activity onset detection. *Ann. Biomed. Eng.*, **35**(9):1532-1538. [doi:10.1007/s10439-007-9320-z]

Miller, L.A., Stubblefield, K.A., Lipschutz, R.D., *et al*., 2008. Improved myoelectric prosthesis control using targeted reinnervation surgery: a case series. *IEEE Trans. Neur. Syst. Rehabil. Eng.*, **16**(1):46-50. [doi:10.1109/TNSRE.2007.911817]

Mummidisetty, C.K., 2009. Analysis of EMG During Clonus Using Wavelets. MS Thesis, University of Miami, Florida, USA.

Parker, P.A., Scott, R.N., 1986. Myoelectric control of prostheses. *Crit. Rev. Biomed. Eng.*, **13**(4):283-310.

Roy, R.R., Hutchison, D.L., Pierotti, D.J., *et al*., 1991. EMG patterns of rat ankle extensors and flexors during treadmill locomotion and swimming. *J. Appl. Physiol.*, **70**(6):2522-2529.

Sabatier, M.J., To, B.N., Rose, S., *et al*., 2011. Chondroitinase ABC reduces time to muscle reinnervation and improves functional recovery after sciatic nerve transection in rats. *J. Neurophysiol.*, **107**(3):747-757. [doi:10.1152/jn.00887.2011]

Solnik, S., de Vita, P., Rider, P., *et al.*, 2008. Teager–Kaiser operator improves the accuracy of EMG onset detection independent of signal-to-noise ratio. *Acta Bioeng. Biomech.*, **10**(2):65-68.

Staude, G., Flachenecker, C., Daumer, M., *et al.*, 2001. Onset detection in surface electromyographic signals: a systematic comparison of methods. *EURASIP J. Adv. Signal Process.*, **2001**:867853. [doi:10.1155/S1110865701000191]

Stubblefield, K.A., Miller, L.A., Lipschutz, R.D., *et al*., 2009. Occupational therapy protocol for amputees with targeted muscle reinnervation. *J. Rehabil. Res. Devel.*, **46**(4):481-488. [doi:10.1682/JRRD.2008.10.0138]

Tysseling, V.M., Janes, L., Imhoff, R., *et al*., 2013. Design and evaluation of a chronic EMG multichannel detection system for long-term recordings of hindlimb muscles in behaving mice. *J. Electromyogr. Kinesiol.*, **23**(3):531-539. [doi:10.1016/j.jelekin.2012.11.014]

von Tscharner, V., 2000. Intensity analysis in time-frequency space of surface myoelectric signals by wavelets of specified resolution. *J. Electromyogr. Kinesiol.*, **10**(6):433-445. [doi:10.1016/S1050-6411(00)00030-4]

Zhou, H., Wu, F.X., Yang, L., *et al.*, 2013. A preliminary analysis of reconstructed nerve function using targeted muscle reinnervation in a rat model. 6th Int. IEEE/EMBS Conf. on Neural Engineering, p.1602-1605.

Zhou, P., Lowery, M.M., Englehart, K.B., *et al.*, 2007. Decoding a new neural machine interface for control of artificial limbs. *J. Neurophysiol.*, **98**(5):2974-2982. [doi:10.1152/jn.00178.2007]